

Mathematical Model Predicting the Critical Heat Flux of Nuclear Reactors

¹Chien-Hsiung Lee, ²Lih-Wu Hourng and ³Kuo-Wei Lin

¹Nuclear Fuels and Materials Division,
Institute of Nuclear Energy Research P.O. Box 3-3,
Lungtan, Taoyuan, 32500, R.O.C., Taiwan

²Department of Mechanical Engineering,
National Central University, Jhongli, 32001, R.O.C., Taiwan

³Department of International Business,
Hsuan Chuang University, Hsinchu, 30092, R.O.C., Taiwan

Received 2012-06-08, Revised 2012-09-14; Accepted 2012-12-12

ABSTRACT

Boiling heat transfer system keeps a nuclear power plant safe without getting over-heated. Crisis will occur if the dissipated heat flux exceeds the critical heat flux value. This study assumes the flow boiling system at high heat flux is characterized by the existence of a very thin liquid layer, known as the “sublayer”, which is trapped between the heated surface and the vapor blankets. In the present study, it is hypothesized that the heat transfer through the liquid sublayer is dominated by the heat conduction and the sublayer is dried out due to occurrence of Helmholtz instability as the relative velocity of the vapor blanket to the local liquid in the sublayer reaches a critical value. By recognizing this hypothesis, a theoretical model for low-quality flow is developed to predict boiling heat transfer and Critical Heat Flux (CHF). To verify the validity of the present model, the predictions are compared with the experimental data of flow boiling heat transfer in the simulation of Pressurized Water Reactor (PWR) and Boiling Water Reactor (BWR) conditions. For the PWR low-quality flow, the comparison demonstrates that the Helmholtz instability is the trigger condition for the onset of CHF.

Keywords: Nuclear Crisis, Critical Heat Flux (CHF), Helmholtz Instability, Boiling Heat Transfer, Boiling Water Reactor (BWR), Pressurized Water Reactor (PWR), Relative Velocity

1. INTRODUCTION

Subcooled or low-quality forced convective boiling system is utilized in the design of nuclear reactor cores, because its high heat fluxes can be dissipated. Therefore, to protect the heated surface from overheating or burnout, a reliable estimation of the boiling heat transfer and its limitation Critical Heat Flux (CHF) is extremely required in the flow boiling system. In general, the boiling heat transfer mechanisms are different at the low heat flux ($q < 0.6$ CHF) and the high heat flux ($q > 0.6$ CHF) as shown in **Fig. 1**. At the former condition, most of the heat flux is provided for nucleation of bubbles (**Fig. 1a**); while at the latter, the boiling heat transfer is dominated by the heat conduction in the liquid sublayer trapped between the heated surface and the vapor blanket (**Fig. 1b**).

In the review of high heat flux boiling mechanisms, many studies have found the existence of liquid sublayer between the heated surface and the bubble layer at high heat flux conditions. Based on the formation of the liquid sublayer, Katto and Yokoya (1968) developed a hydrodynamic model near the CHF according to the consumption of liquid film.

Through a measurement of the transient variation of heated surface temperature during nucleate pool boiling of water, Chi-Liang and Mesler (1977) confirmed the existence of a liquid film beneath the growing vapor which is paramount in transferring heat. Bhat *et al.* (1983) hypothesized that the heat transfer, in the high heat flux region between 0.6 CHF and CHF, takes place mainly due to the heat conduction through the liquid layer formed on the heated surface.

Corresponding Author: Kuo-Wei Lin, Department of International Business, Hsuan Chuang University, Hsinchu, 30092, R.O.C., Taiwan

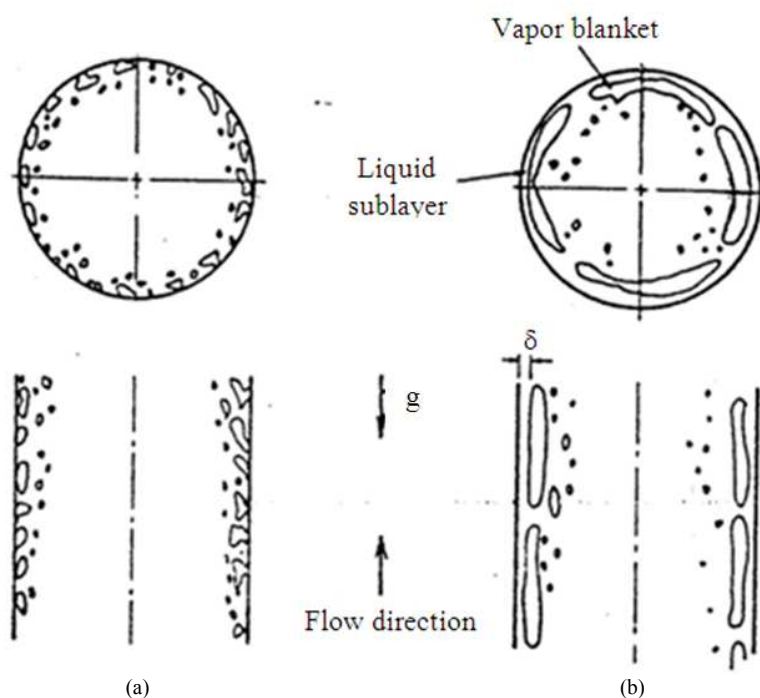


Fig. 1. Liquid-vapor configuration for up-flow boiling water (a) low heat flux condition ($<0.6\text{ CHF}$) (b) high heat flux condition ($>0.6\text{ CHF}$)

In a subsequent paper of Bhat *et al.* (1986), experimental results of sublayer thickness and frequency of vapor mass show good agreement with their previous predictions. Later, many high heat flux models based on heat conduction in the liquid layer have been reported (Chinnm *et al.*, 1989; Jairajpuri and Saini, 1991; Rajvanshi *et al.*, 1992). Although all the available models are developed specifically for pool boiling, Chinnm *et al.* (1989) expected that the same concept of heat conduction through the sublayer may also be applied to flow boiling conditions.

The sublayer concept with heat balance rather than heat conduction has also been applied in the research of flow boiling for predicting the CHF. For example, Haramura and Katto (1983), as one of the pioneers of the sublayer dry out theory, originally derived a high heat flux model, based on the heat balance of liquid film located between the heated surface and a vapor blanket, to predict the flow boiling CHF on flat plates. Lee and Mudawwar (1988) postulated that CHF occurs when the liquid film underneath the vapor blanket dries out due to the oscillation motion of the blanket for an internal flow boiling system. They emphasized that the onset of

sublayer dry out was triggered by Helmholtz instability in the sublayer-vapor blanket interface while as the length of the vapor blanket is equal to the Helmholtz critical wavelength. Later, by replacing the single-phase fluid properties with the two-phase homogeneous equilibrium fluid properties, Lin *et al.* (1988a; 1988b) made an improved sublayer dry out model to extend the applicable range from the subcooled flow boiling to the low-quality saturated flow boiling. By accounting for the passage time of the blanket, Katto (1990a; 1990b; 1992) used the similar idea yet different approach to evaluate the DHF required to vaporize the liquid film underneath the blanket. Celata (1991) suggested that this mechanism may also be applied in the thermal-hydraulics studies of high heat flux, high mass flow rate fusion reactor.

Although thickness of liquid sublayers calculated by Lee and Mudawwar (1988) and Katto (1990a; 1990b; 1992) models are quite different, it is worth to note that the magnitude of sublayer thickness is extremely tiny (order of $10^{-7}\sim 10^{-3}\text{m}$). It is thus appropriate to hypothesize that the convective boiling heat transfer is dominated by the heat conduction through the liquid sublayer at superheated conditions. Therefore, based on heat conduction in the sublayer, Lin *et al.* (1994)

developed a theoretical model for subcooled flow boiling heat transfer at high heat flux conditions.

Lee and Lin (1993) conducted the flow transient CHF experiments in the simulation of Pressurized Water Reactor (PWR) conditions. The experimental data were compared with the predictions of improved model by Lin *et al.* (1988a).

Their results reveal that the sublayer dry out model is appropriate. All of the afore-mentioned theoretical approaches for predicting the flow boiling CHF (Lee and Mudawwar, 1988; Lin *et al.*, 1988a; 1988b; Katto, 1990a; 1990b; 1992) acknowledged that the sublayer dry out is triggered by Helmholtz instability at the sublayer-vapor blanket interface. However, so far there is no theoretical model based on the Helmholtz instability concept proposed for prediction of occurrence of CHF. In the present study, a critical condition for onset of CHF is derived based on the Helmholtz instability at interface of two streams. The relative velocity of two streams is calculated using the heat transfer model by Lin *et al.* (1994). The predicted transient time to the onset of CHF provided reasonable agreement with the Lee and Lin (1993) experimental data.

2. MATERIALS AND METHODS

Based on the boiling configuration of subcooled flow through a vertical tube at the high heat flux conditions as shown in **Fig. 1b**, a theoretical boiling heat transfer model was proposed with the following assumptions:

- In the subcooled flow through a vertical tube, the vapor blankets are formed from small bubbles piling up as vertical distorted vapor cylinders. All the vapor blankets glide up parallel to the heated wall and shield the heated wall from the cooling of bulk flow. As a result, a liquid sublayer forms between the vapor blankets and the heated wall
- For high heat flux, the passing period of the vapor blanket becomes sufficiently long as that reported in Hino and Ueda (1985) investigation. Thus, the sublayer seems always exist between the heated wall and the vapor blanket
- Since the thickness of the sublayer is very thin with low flow rate, it is reasonable to assume that, in the sublayer, the bubble generation is ceased and the heat convection can be ignored due to small velocity, the heat transfer across the liquid sublayer is dominated by heat conduction

Figure 2 shows the temperature distribution in the sublayer and the force balance on the vapor blanket. As mentioned above, the q heat flux can be calculated by

heat conduction through the thickness of sublayer δ with the temperature difference of heated wall T_w and the vapor blanket T_{sat} . i.e.:

$$q = \frac{k_f(T_w - T_{sat})}{\delta} \quad (1)$$

In this equation k_f is the conductivity of liquid. By Newton's law of cooling, the heat flux also can be expressed as:

$$q = h(T_w - T_b) \quad (2)$$

From Eq. 1 and 2, the subcooled boiling heat transfer coefficient h can be obtained as Eq. 3:

$$h = q / (q\delta / k_f + T_{sat} - T_b) \quad (3)$$

Thus to determine the heat transfer coefficient, it is needed to calculate the sublayer thickness δ which can be obtained by force balance on the vapor blanket in the axial and the radial directions (**Fig. 2**). For the two-phase flow, the effective fluid properties such as density ρ and viscosity μ need to be modified first.

2.1. Effective Homogeneous Fluid Properties

The homogeneous two-phase flow model is assumed to be suitable for the present subcooled or low-quality flow boiling conditions.

2.2. Magnitude of True Quality

The true quality x can be evaluated by using Saha and Zuber (1974) formula Eq. 4:

$$x = \frac{x_e - x_d \exp(x_e / x_d - 1)}{1 - x_d \exp(x_e / x_d - 1)} \quad (4)$$

where, x_e is the thermodynamic equilibrium quality and x_d is the thermodynamic quality at the point of bubble detachment from that heated wall. The value of x_d is Eq. 5:

$$x_d = -0.0022 \frac{q c_{pf} D}{H_{fg} k_f}; \text{ for } Pe_f < 70000 \quad (5)$$

$$x_d = -154 \frac{q}{H_{fg} G}; \text{ for } Pe_f > 70000$$

where, c_{pf} the specific heat capacity of liquid, D the inner diameter of the tube, H_{fg} is the latent heat of vaporization, G the mass velocity and Pe_f the Peclet number of liquid. Note that, as $x_e \leq x_d$ the true quality is identically zero for the single-phase flow.

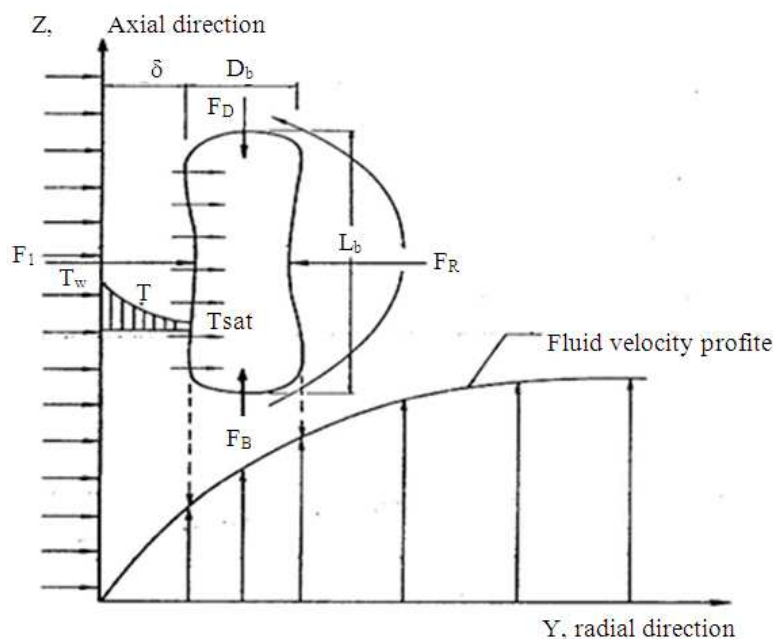


Fig. 2. Schematic diagram of vapor blankete moving in vertical turbulent flow at high heat flux condition

2.3. ρ and μ for Homogeneous Flow

For the homogeneous two-phase flow of true quality x , the fluid density ρ is generally given by Eq. 6:

$$\frac{1}{\rho} = \frac{x}{\rho_f} + \frac{(1-x)}{\rho_g} \tag{6}$$

In this equation ρ_g and ρ_f respectively, denote the density of vapor and liquid, while the mean two-phase viscosity μ will be evaluated by using the formula of Dukler *et al.* (1964) Eq. 7:

$$\mu = \rho[x\mu_g v_g + (1-x)\mu_f v_f] \tag{7}$$

where, μ_g and μ_f represent the viscosity of vapor and liquid; and v_g and v_f are specific volume of vapor and liquid, respectively.

2.4. Relative Velocity of Vapor Blanket to Liquid

At high heat flux condition, the vapor blanket is formed by the coalescence of small bubbles. The vapor blanket is assumed to be a distorted cylinder of length L_b and D_b diameter, which forms a flat interface near the wall. Consider the force balance in the axial direction, the relative velocity of the blanket with respect to the liquid will be determined by a balance between the buoyancy force F_b and the drag force F_d Eq. 8 and 9:

$$F_B + F_D = 0 \tag{8}$$

Where:

$$F_B = \frac{\pi}{4} D_b^2 L_b \Delta \rho g \tag{9}$$

And:

$$F_D = -\frac{1}{2} \rho_f C_D U_{bl} \frac{2\pi D_b^2}{4} \tag{10}$$

in which $\Delta \rho = \rho_f - \rho_g$ is the density difference between the two phases, C_D the drag coefficient and U_{bl} the relative velocity of the vapor blanket with respect to the liquid at the position corresponding to the centerline of the blanket. The negative sign in Eq. 10 indicates that the direction of the drag force is opposite to the flow direction. Chan and Prince (1965) proposed an expression of the drag coefficient for a small deformed bubble Eq. 11:

$$C_D = \frac{48\mu_f}{\rho_f D_{eb} U_{bl}} \tag{11}$$

Since the vapor blanket is formed initially by the coalescence a vertical column of small bubbles, the

equivalent diameter D_{eb} and D_b are assumed to be equal to the bubble departure diameter (Lee and Mudawwar, 1988) and the latter can be obtained from the correlation of Cole and Rohsenow (1968) Eq. 12:

$$D_b 1.5 \times 10^{-4} \left(\frac{\sigma}{g\Delta\rho} \right)^{0.5} \left(\frac{\rho_f C_{pf} T_{sat}}{\rho_g H_{fg}} \right)^{1.25} \quad (12)$$

where, σ is the surface tension. Weisman and Pei (1983) indicated that the bubbles are approximately ellipsoidal with the ratio of long to short ellipse axis being about 3:1 in the case of high heat flux. So the length of the vapor blanket L_b is assumed to be three times of the bubble diameter D_b . Combining Eq. 8 through (12) with the relations $D_{eb}=D_b$ and $L_b=3D_b$ gives the relative velocity of the bubble with respect to the liquid as Eq. 13:

$$U_{bl} = \frac{(\rho_f - \rho_g) D_b^2 g}{8\mu_f} \quad (13)$$

2.5. Liquid Velocity Gradient

The local liquid velocity gradient can be evaluated by the force balance of a vapor blanket in the radial direction and the velocity profile distribution.

2.6. Force Balance in Radial Direction

The force balance of a vapor blanket in the radial direction is shown as **Fig. 2**. Vapro generation due to sublayer evaporation creates a rate of change of momentum F_1 which pushes the vapor blanket away from the wall. However, the lateral motion of the blanket is resisted by a lateral force F_R caused by the vapor blanket rotation, which is resulted due to the velocity gradient associated with the liquid boundary layer in the tube. The inertial force F_1 is given by Eq. 14:

$$F_1 = \rho_g V_b^2 D_b L_b \quad (14)$$

where, V_b is the vapor velocity due to evaporation of the sublayer and can be expressed as Eq. 15:

$$V_b = q / (\rho_g H_{fg}) \quad (15)$$

Beyerlein *et al.* (1985) derived an expression for the lateral force on a bubble in turbulent two-phase flow in a vertical tube. The lateral force on the vapor blanket is determined by the relative velocity of the blanket and the gradient of the liquid velocity profile, i.e Eq. 16:

$$F_R = -C_{pf} U_{bl} \frac{\partial U_L}{\partial y} \frac{\pi}{4} D_b^2 L_b \quad (16)$$

where, U_L is the local liquid velocity and C is a parameter which accounts for the effects of turbulent fluctuations and local bubble concentration on the rotation of the vapor blanket.

From a liquid-gas two-phase flow experiment in the adiabatic boundary condition, Beyerlein *et al.* (1985) found that C is a function of the average void fraction and the liquid Reynolds number. In the present model for vapor-liquid system with wall heating, the dependences of two-phase Reynolds number and the boiling number in the parameter C are taken into account and is modeled by Eq. 17:

$$C = a_1 Re^{a_2} Bo_*^{a_3} \quad (17)$$

In which a_1 , a_2 and a_3 are empirical constants, $Re = GD/\mu$ is the effective Reynolds number for homogeneous flow and Bo_* is a modified boiling number defined as Eq. 18:

$$Bo_* = \frac{q}{H_{fg} \left(G \frac{1-x}{1-\alpha} \right)} = Bo[(1-x)/1-\alpha] \quad (18)$$

In which $Bo = q/(GH_{fg})$ is the conventional boiling number and α is the void fraction Eq. 19:

$$\alpha = v_g x / [v_g x + v_f(1-x)] \quad (19)$$

Upon combining the above equations, the liquid velocity gradient $\partial U_L / \partial y$ can be evaluated as the values of a_1 , a_2 and a_3 are treated known quantities, it is Eq. 20:

$$\frac{\partial U_L}{\partial y} = \frac{32\mu_f q^2}{g\pi C_{pf} \rho_g (\rho_f - \rho_g) H_{fg}^2 D_b^3} \quad (20)$$

2.7. Velocity Profile Distribution

Applying the Karman's three-layer structure of turbulent flow in a tube, the friction velocity U^+ can be derived by the non-dimensional wall distance y^+ , that is Eq. 21a-d:

$$U^+ = y^+ ; \text{for } 0 < y^+ < 5 \quad (21a)$$

$$U^+ = 5.0 \ln y^+ - 3.05 ; \text{for } 5 \leq y^+ \leq 30 \quad (21b)$$

$$U^+ = 2.5 \ln y^+ + 5.5 ; \text{for } 30 < y^+ \quad (21c)$$

Where:

$$U^+ = U / \sqrt{\tau_w / \rho}, \quad y^+ = y \sqrt{\tau_w \rho / \mu} \quad (21d)$$

And τ_w is wall shear stress which can be obtained by Eq. 22:

$$\tau_w = f \rho \frac{(G / \rho)^2}{2} \quad (22)$$

where, the friction factor f is the fanning friction factor, can be calculated by Eq. 23:

$$F = 0.046 \text{Re}^{-0.2} \quad (23)$$

The effective value of the velocity gradient causing vapor blanket rotation can be approximated as velocity gradient at the radial position of $\delta + D_b/2$ from the wall. Lee and Mudawwar (1988) found that the liquid velocity profile around the vapor blanket locates in the buffer region and the effective velocity gradient can be calculated from Eq. (21a-d):

$$\frac{\partial U_{\perp}}{\partial y} = 5 \sqrt{\tau_w / \rho} \left(\frac{1}{\delta + (D_b / 2)} \right) \quad (24)$$

2.8. Thickness of Sublayer

Comparing Eq. 20 and 24, the thickness of sublayer δ is obtained by:

$$\delta = \frac{S \pi \sqrt{\tau_w / \rho} g C_{pf} \rho_g (\rho_f - \rho_g) H_{fg}^2 D_b^2 - \frac{D_b}{2}}{32 \mu f q^2} \quad (25)$$

Thus, the heat transfer coefficient h can be predicted by substituting Eq. 25 into Eq. 3.

2.9. Velocity of Vapor Blanket

To determine the onset of CHF, it is needed to calculate the velocity of vapor blanket U_b which can be approximated as the superposition of the local liquid velocity at the radial position of $\delta + D_b/2$ from the wall and the relative vapor blanket velocity. Therefore, the velocity of the vapor blanket can be calculated from Eq. 21b and 13, it is Eq. 26:

$$U_b = \sqrt{\frac{\tau_w}{\rho}} \left\{ 5.0 \ln \left[\frac{(\delta + D_b / 2) \sqrt{\tau_w / \rho}}{\mu} \right] - 3.05 \right\} + \frac{(\rho_f - \rho_g) D_b^2 g}{8 \mu_f} \quad (26)$$

2.10. Critical Velocity for Onset of CHF

Figure 3 represents the flow boiling configuration of subcooled or low-quality flow immediately just before and occurrence of CHF. This phenomenon is called Helmholtz instability which causes a wavy motion of the sublayer-vapor blanket interface. Based on the concept of Helmholtz instability as the relative velocity of the two streams, i.e., the liquid in the sublayer and the vapor in the vapor blanket, reaches a critical value, a wavy motion of the interface is induced. Due to the instability nature, the amplitude of the wavy motion can be amplified. The critical value will be evaluated based on the following assumptions:

- The length of the blanket changes suddenly to the Helmholtz critical wavelength when the vapor blanket velocity reaches the critical value and the sublayer also adjust its thickness
- The vapor blanket touches the heated surface as result of the Helmholtz instability, the dry patch persists and spreads very quickly, which induces a sudden rise in wall temperature
- CHF occurs when the rate of sublayer mass loss by evaporation exceeds the mass flow rate of the liquid entering the sublayer from the core region

2.11. Thickness of Sublayer

Since CHF is postulated to occur as a result of Helmholtz instability, the length of the sublayer and the vapor blanket are assumed to be equal to the Helmholtz critical wavelength L_{bH} , as shown in **Fig. 3a**, i.e Eq. 27:

$$L_{bH} = \frac{2 \pi \sigma (\rho_f + \rho_g)}{\rho_f \rho_g (U_{bH} - U_m)^2} a \quad (27)$$

In which U_{bH} , is the critical velocity of the vapor blanket to onset of CHF, U_m the liquid velocity in the sublayer. Since U_{bH} is always much higher than U_m , the above expression can be reduced to:

$$L_{bH} = \frac{2 \pi \sigma (\rho_f + \rho_g)}{\rho_f \rho_g U_{bH}^2} \quad (28)$$

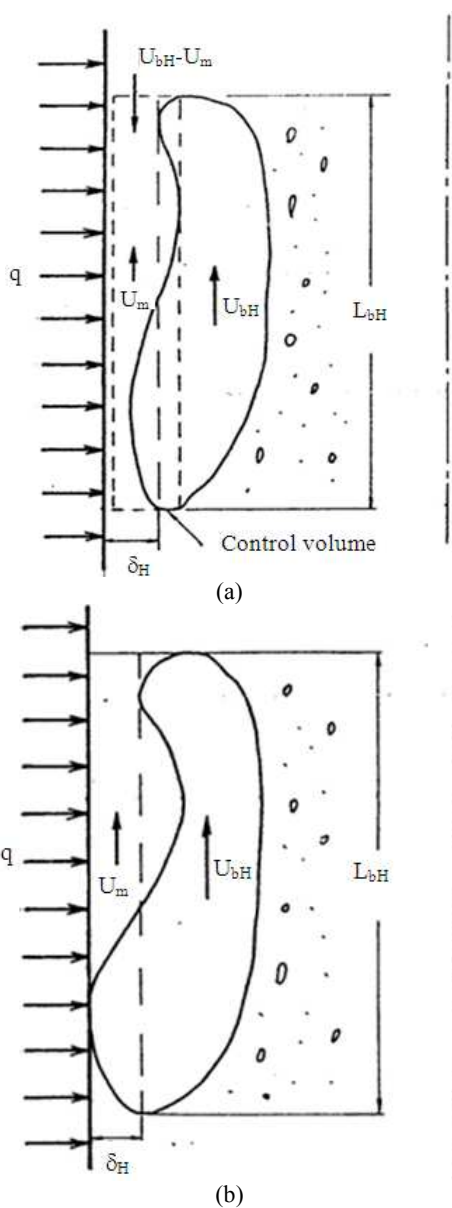


Fig. 3. The proposed sublayer dry out mechanism (a) Just before CHF (b) Occurrence of CHF

Since the occurrence of CHF is a result of local sublayer dry out, the minimum critical heat flux q_c necessary to evaporate the mass flux in the sublayer (see Fig. 3a) is:

$$q_c L_{bH} = G_m \delta_H [H_{fg} + C_{pf}(T_{sat} - T_m)] \quad (29)$$

where, δ_H is the thickness of the sublayer to onset of CHF, T_m the temperature of the liquid entering the

sublayer, G_m the liquid mass flux flowing into the sublayer, can be express as Eq. 30:

$$G_m = \rho f(U_{bH} - U_m) \cong \rho_f U_{bH} \quad (30)$$

Since $H_{fg} = C_{pf}$ and in general, $T_{sat} = T_m$ the second term in RHS of Eq. 29 can be neglected. Therefore, combining Eq. 28 through (30) gives δ_H the thickness of the sublayer as Eq. 31:

$$\delta_H = \frac{2\pi\sigma q_c (\rho_f + \rho_g)}{\rho_f^2 \rho_g H_{fg} U_{bH}^3} \quad (31)$$

2.12. Relative Velocity of Capor Blanket to Liquid

Near the CHF condition, the relative velocity of the vapor blanket to local liquid U_{bLH} can be determined by a balance between the buoyancy force F_B and the drag force F_D Eq. 33 and 34:

$$F_B + F_D = 0 \quad (32)$$

Where:

$$F_B = \frac{\pi}{4} D_b^2 L_{bH} (\rho_f - \rho_g) g \quad (33)$$

And:

$$F_D = -\frac{1}{2} \rho_f C_D U_{bLH}^2 \frac{\pi D_b^2}{4} \quad (34)$$

In which C_D is the drag coefficient, can be evaluated through the Chan and Prince (1965) Eq. 35:

$$C_D = \frac{48\mu_f}{\rho_f D_b U_{bLH}} \quad (35)$$

Combining Eq. 28 and 32 through 35 gives the relative velocity of the vapor blanket:

$$U_{bLH} = \frac{\pi\sigma(\rho_f^2 - \rho_g^2)D_b g}{12\mu_f \rho_f \rho_g U_{bH}^2} \quad (36)$$

2.13. Critical Velocity of Vapor Blanket

The critical velocity of the vapor blanket is derived by the supersession of local liquid velocity at the radial position of $\delta_H + D_b/2$ from the wall and the blanket relative velocity U_{bH} which can be obtained from Eq. 21b and 36. it is Eq. 37:

$$U_{bh} = \sqrt{\frac{\tau_w}{\rho}} \left\{ 5.0 \ln \left[\frac{\left(\frac{2\pi\sigma q_c (\rho_f + \rho_g) + D_b}{\rho_f^2 \rho_g H_{fg} U_{bh}^3} + \frac{D_b}{2} \right) \sqrt{\tau_w \rho}}{\mu} \right] - 3.05 \right\} + \frac{\pi\sigma(\rho_f^2 - \rho_g^2)D_b g}{12\mu_f \rho_f \rho_g U_{bh}^2} \quad (37)$$

Thus, the critical blanket velocity U_{bh} can be predicted by the numerical iteration.

3. RESULTS AND DISCUSSION

3.1. Verification of Heat Transfer Model

By a regression analysis of 321 experimental data in the simulation of Light Water Reactors (LWRs) conditions ($P = 6.9\sim 15.5\text{MPa}$), that is conducted by Lin *et al.* (1994), empirical constants a_1 , a_2 and a_3 are found to be 0.50, 1.20 and 2.21, respectively, **Fig. 4** provides a comparison of predicted and experimental heat transfer coefficient for subcooled flow boiling at high heat flux ($0.6 \text{ CHF} < q < \text{CHF}$). The predictions agree well with the experimental data and the majority of data points fall within the error band of 40%.

Gungor and Winterton (1986) evaluated the various correlations for subcooled flow boiling, by comparing with measured data, they reported that the correlations by Moles and Shaw (1972); Shah (1977) and Gungor and Winterton (1986) are the best ones among others. Therefore, the above mentioned three correlations are selected in the study of subcooled flow boiling heat transfer coefficients. The comparison of these correlations with the experimental data is in **Table 1**. The correlations by Moles and Shaw (1972) and Gungor and Winterton (1986) that performed well with the high pressure (6.9MPa~15.5 MPa) boiling data give mean deviation of 32.7% (Moles and Shaw, 1972) and 46.1% (Gungor and Winterton, 1986), this error is closed to the report for subcooled flow boiling data at the pressure from 13.2 to 20.3 MPa.

The correlation by Moles and Shaw present a better agreement with the experimental data within average deviation of 23.9% and mean deviation of 32.7%. However, this correlation is derived by direct dimensionless analysis and no significant physical meanings. Since the present model is developed based on the high heat flux mechanisms of vapor blanket and heat conduction in sublayer, it is superior to other correlations.

3.2. Verification of Steady-State CHF

To verify the trigger condition for onset of CHF, it is needed to examine the comparison between the critical value U_{bh} and the vapor blanket velocity U_b as CHF occurs.

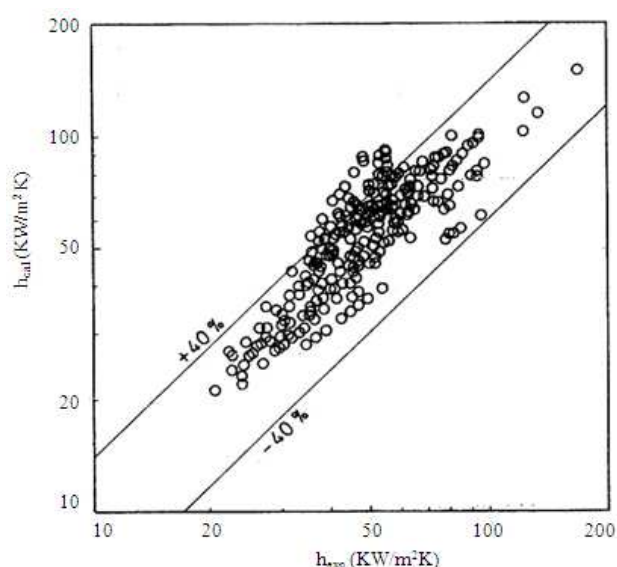


Fig. 4. Comparison of the predicted heat transfer coefficient with the experimental data at high heat flux

Table 1. The statistical results for predicting boiling heat transfer coefficient by the various correlation

Correlation	Number of points	AD(%)	MD(%)
Gungor and Interton	321	45.4	46.1
Moles and Shaw	321	23.9	32.7
Shah	321	75.4	76.0
Present model	321	12.6	18.6

Therefore, an analysis of relation between U_{bh} and U_b will be study based on a total of 362 data points of subcooled and low-quality saturated flow boiling water included in the tabular CHF data of the USSR Academy of Sciences (Collier, 1981), at the conditions of $P = 6.9\sim 17.6\text{MPa}$, $G = 1000\sim 5000 \text{ kg m}^{-2}\text{s}$ and $\alpha = 0\sim 0.7$. The analysis provided the Average Deviation (AD) of 5.3% and mean deviation of 22.8%. Thus, based on the Helmholtz instability at the sublayer-vapor blanket interface is the trigger condition for the onset of CHF as the blanket velocity reaches a critical value, this hypothesis is appropriate.

3.3. Verification of Tr0061nsient CHF

Lee and Lin (1993) conducted an experiment flow transient CHF in the simulation of PWR at the linear mass flow decay rate from 0.1 to 30%/s. **Figure 5** shows the variation of the inflow mass velocity and the wall temperature with the transient time at the flow decay rate of 0.1%/s. The onset of CHF is determined at the exit of the test section while the wall temperature excursion occurred, since the abrupt drop and the followed jump in wall temperature implies rewetting and dry out process of liquid film underneath the vapor blanket.

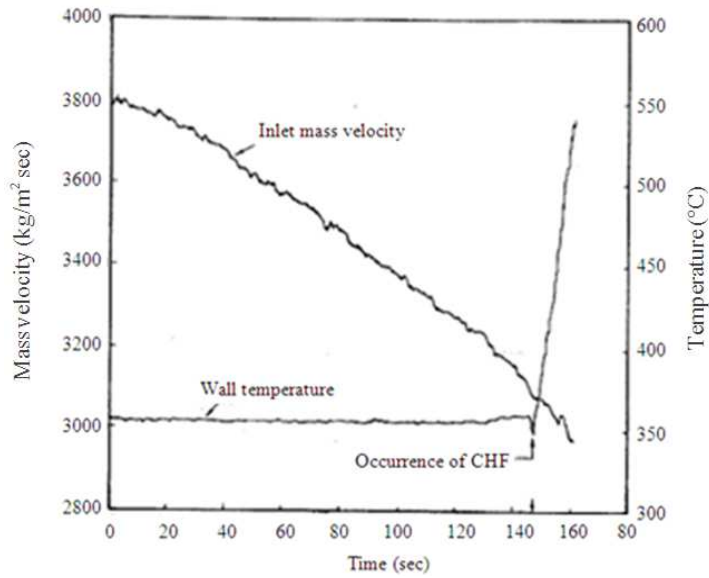


Fig. 5. The variation of the inflow mass velocity and the wall temperature with the transient time at the flow decay rate of 0.1%/s

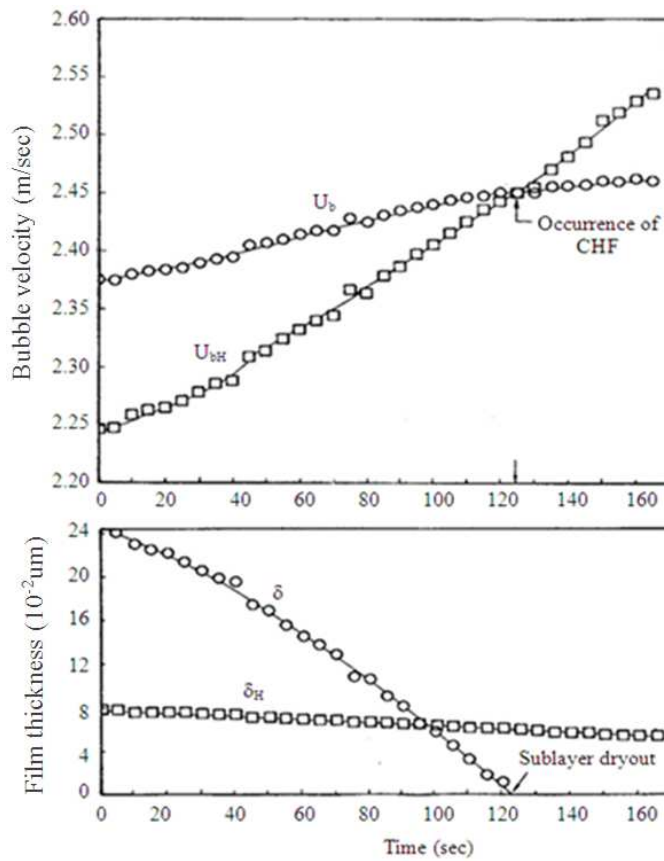


Fig. 6. The variation of sublayer thickness and vapor blanket velocity with the transient time at the flow decay rate of 0.1%/s

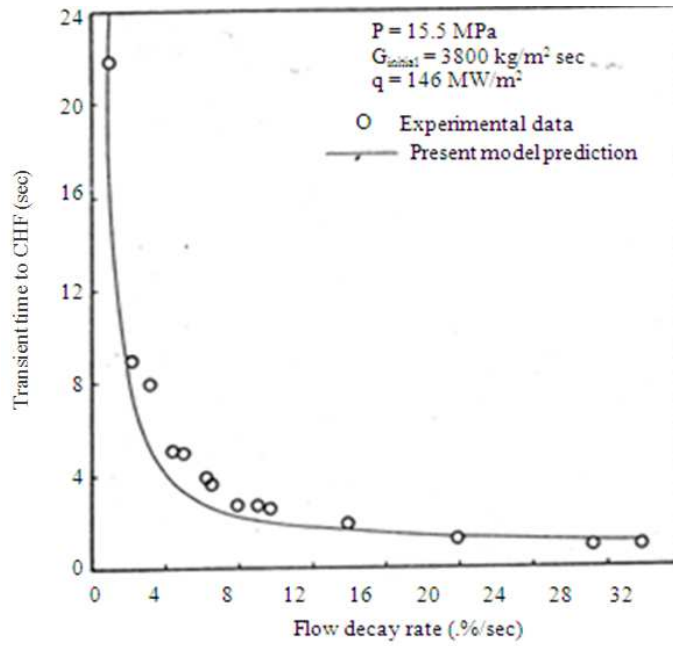


Fig. 7. The relation between the transient time to CHF and the flow decay rate

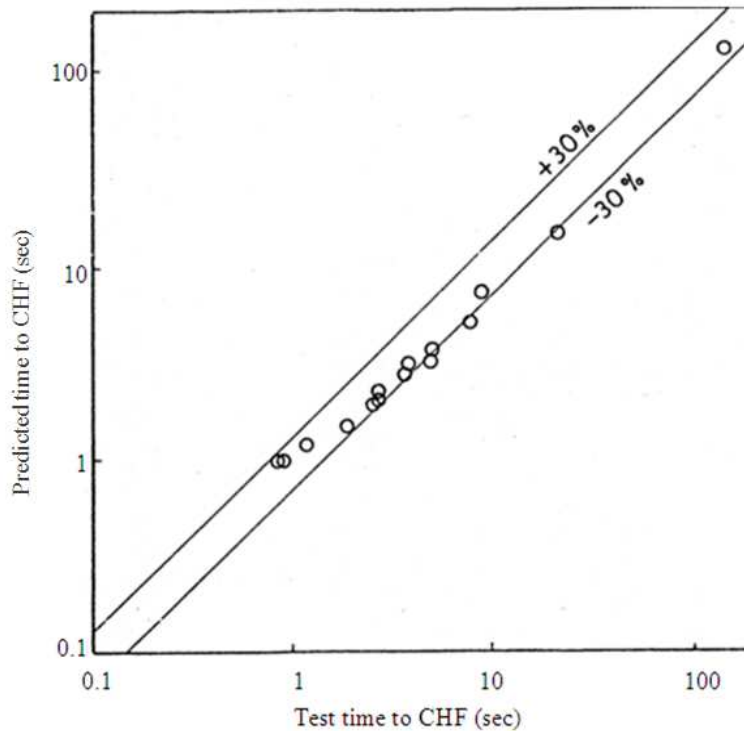


Fig. 8. Comparison of the predicted time to CHF with the experimental data under simulating PWR flow transient

Table 2. The statistical results for predicting transient time to CHF by the various correlations

Correlation	No. of points	AD(%)	MD(%)
EPRI-1	15	-40.8	-40.8
BandW-2	15	-12.2	13.9
Lin, Lee and Pei	15	-25.7	-25.7
Present model	15	-17.8	20.6

The experimental data will be compared with present model predictions. In present study, the predicted time to onset of CHF is determined as the blanket velocity is reached the critical velocity.

Figure 6 show the variation a vapor blanket velocity and sublayer thickness with the transient time at the conditions of $T_{in} = 290^{\circ}\text{C}$, $P = 15.5\text{MPa}$, $G_{initial} = 3800\text{ kg m}^{-2}\text{ sec}$ and flow decay rate $=0.1\%/s$. The CHF is occurred when U_b is equal to U_{bH} , it is worth to note that the thickness of sublayer is very near zero during the occurrence of CHF, this is a good evidence for sublayer dry out model. In **Fig. 7**, as the flow decay rate increase from 0.1-30%/s, it is shown that the experimental and the predicted transient time to CHF is decreased. **Figure 8** provides a comparison of the predicted and measured time to ones of CHF. The prediction agrees well with the experimental data and the majority of data points fall within the error bank of 30%

The well-known CHF correction of BandW-2 (Gellerstedt, 1969), EPR-1 (Fighetti and Reddy, 1983) and Lin *et al.* (1988a) are used to predict the onset of CHF in comparison with the present model. The comparison is shown in **Table 2**. Only the BandW-2 correlation with 13.9% of mean deviation is better than the prediction of present model. But the process from boiling heat transfer to the onset of CHF only can be demonstrated by the present model, this is why the present model is superior to the other correlations.

4. CONCLUSION

A theoretical model based on the Helmholtz instability has been developed for the evaluation of heat transfer performance and occurrence of CHF in low-quality flow boiling problem. For prediction of the heat transfer coefficient and the critical heat flux, the validity of the present model has been demonstrated by comparing with the existing experimental data and empirical corrections. However, it is worthy to note that the present model is developed based on the flow and heat transfer mechanisms. Therefore, unlike most of the previous models, the present one is of more physical meanings. It is believed that the present theoretical

model is also useful to the analysis of the cooling technology related to the flow boiling heat transfer.

5. REFERENCES

1. Beyerlein, S.W., R.K. Cossman and H.J. Richter, 1985. Prediction of bubble concentration profiles in vertical turbulent two-phase flow. *Int. J. Mul. Flow*, 11: 629-641. DOI: 10.1016/0301-9322(85)90083-7
2. Bhat, A.M., J.S. Saini and R. Prakash, 1986. Role of macrolayer evaporation in pool boiling at high heat flux. *Int. J. Heat Mass Trans.*, 29: 1953-1961. DOI: 10.1016/0017-9310(86)90014-1
3. Bhat, A.M., R. Prakash and J.S. Saini, 1983. Heat transfer in nucleate pool boiling at high heat flux. *Int. J. Heat Mass Trans.*, 26: 833-840. DOI: 10.1016/S0017-9310(83)80107-0
4. Celata, G.P., 1991. A review of recent experiments and predictions aspects of burnout at very high heat fluxes. *Proceedings of the International Journal Multiphase Flows Conference, (IJMFC' 91)*, pp: 31-40.
5. Chan, B.K.C. and R.G.H. Prince, 1965. Distillation studies-viscous drag on a gas bubble rising in a liquid. *AICHE, J.* 11: 176-192. DOI: 10.1002/aic.690110139
6. Chi-Liang, Y. and R.B. Mesler, 1977. A study of nucleate boiling near the peak heat flux through measurement of transient surface temperature. *Int. J. Heat Mass Trans.*, 20: 827-840. DOI: 10.1016/0017-9310(77)90112-0
7. Chinm, P., J.Y. Hwang and T.L. Lin, 1989. The mechanism of heat transfer in transition boiling. *Int. J. Heat Mass Trans.*, 32: 1337-1349. DOI: 10.1016/0017-9310(89)90033-1
8. Cole, R. and W.R. Rohsenow, 1968. Correlation of bubble departure diameters for boiling of saturated liquids. *Proceedings of the Chemical Enginring Progress Symposym, (CEPS' 68)*, pp: 211-213.
9. Collier, J.G., 1981. *Convective Boiling and Condensation*. 2nd Edn., McGraw-Hill, New York, ISBN-10: 0070117985, pp: 435.
10. Dukler, A.E., M. Wicks and R.G. Cleveland, 1964. Frictional pressure drop in two-phase flow: B. An approach through similarity analysis. *AICHE J.*, 10: 38-51. DOI: 10.1002/aic.690100118

11. Fighetti, C.F. and D.C. Reddy, 1983. Parametric study of CHF data.
12. Gellerstedt, J.S., R.A. Lee, W.J. Oberjohn, R.H. Wilson and L.J. Stanek, 1969. Correlation of critical heat flux in a bundle cooled by pressurized water reactor.
13. Gungor, K.E. and R.H.S. Winterton, 1986. A general correlation for flow boiling in tubes and annuli. *Int. J. Heat Mass Trans.*, 29: 351-358. DOI: 10.1016/0017-9310(86)90205-X
14. Haramura, Y. and Y. Katto, 1983. A new hydrodynamic model of critical heat flux, applicable widely to both pool and forced convection boiling on submerged bodies in saturated liquids. *Int. J. Heat Mass Trans.*, 26: 389-399. DOI: 10.1016/0017-9310(83)90043-1
15. Hino, R. and T. Ueda, 1985. Studies on heat transfer and flow characteristics in subcooled flow boiling-part 2. flow characteristics. *Int. J. Multiphase flow*, 11: 283-297. DOI: 10.1016/0301-9322(85)90059-X
16. Jairajpuri, A.M. and J.S. Saini, 1991. A new model for heat flow through macrolayer in pool boiling at high heat flux. *Int. J. Heat Mass Trans.*, 34: 1579-1591. DOI: 10.1016/0017-9310(91)90138-5
17. Katto, Y. and S. Yokoya, 1968. Principal mechanism of boiling crisis in pool boiling. *Int. J. Heat Mass Tran.*, 11: 993-1002. DOI: 10.1016/0017-9310(68)90005-7
18. Katto, Y., 1990a. A physical approach to critical heat flux of subcooled flow boiling in round tubes. *Int. J. Heat Mass Trans.*, 33: 611-620. DOI: 10.1016/0017-9310(90)90160-V
19. Katto, Y., 1990b. Prediction of critical heat flux of subcooled flow boiling in round tubes. *Int. J. Heat Mass Trans.*, 33: 1921-1928. DOI: 10.1016/0017-9310(90)90223-H
20. Katto, Y., 1992. A prediction model of subcooled water flow boiling CHF for pressure in the range 0.1-20 MPa. *Int. J. Heat Mass Trans.*, 35: 115-1123. DOI: 10.1016/0017-9310(92)90172-O
21. Lee, C.H. and I. Mudawwar, 1988. A mechanistic critical heat flux model for subcooled flow boiling based on local bulk flow conditions. *Int. J. Mul. flow*, 14: 711-728. DOI: 10.1016/0301-9322(88)90070-5
22. Lee, C.H. and K.W. Lin, 1993. Experimental investigation of flow transient critical heat flux at light water reactor conditions. *Int. Commun. Heat Mass Trans.*, 20: 477-488. DOI: 10.1016/0735-1933(93)90060-9
23. Lin, K.W., C.H. Lee, L.W. Hourng and J.C. Hsu, 1994. A theoretical and experimental study on subcooled flow boiling at high heat flux. *Warme-und Stoffubertragung*, 29: 319-327. DOI: 10.1007/BF01578416
24. Lin, W.S., B.S. Pei, C.H. Lee and I.A. Mudawwar, 1988b. A mechanistic critical heat flu critical heat flux model for rod bundles under pressurized water reactor conditions. *Int. J. Mul. Flow.*, 14: 711-728. DOI: 10.1016/0301-9322(88)90070-5
25. Lin, W.S., C.H. Lee and B.S. Pei, 1988a. An improved theoretical critical heat flux model for low-quality flow. *Nuclear Technol.*, 88: 291-336. www.osti.gov/energycitations/product.biblio.jsp?osti_id=6969153
26. Moles, F.D. and J.F.G. Shaw, 1972. Boiling heat transfer to subcooled liquids under conditions of forced convection. *Trans. Inst. Chem. Eng.*, 50: 76-84.
27. Rajvanshi, A.K., J.S. Saini and R. Prakash, 1992. Investigation of macrolayer thickness in nucleate pool boiling at high heat flux. *Int. J. Heat Mass Trans.*, 35: 343-350. DOI: 10.1016/0017-9310(92)90272-T
28. Saha, P. and N. Zuber, 1974. Point of net vapor generation and vapor void fraction in subcooled boiling. *Proceedings of the 5th International Heat Transfer Conference, (IHTC' 74), Tokyo, Japan*, pp: 175-179.
29. Shah, M.M., 1977. A general correlation for heat transfer during subcooled boiling in pipes and annuli. *Ashrae Trans.*, 83: 202-217. www.mmshah.org/publications/SHAH%20SC%20BOIL%20CORR%201977.pdf
30. Weisman, J. and B.S. Pei, 1983. Prediction of critical heat flux in flow boiling at low qualities. *Int. J. Heat Mass Trans.*, 26: 1463-1477. DOI: 10.1016/S0017-9310(83)80047-7